JCI insight

Treg gene signatures predict and measure type 1 diabetes trajectory

Anne M. Pesenacker, … , Scott J. Tebbutt, Megan K. Levings

JCI Insight. 2019. https://doi.org/10.1172/jci.insight.123879.

Clinical Medicine In-Press Preview Endocrinology Immunology

BACKGROUND. Multiple therapeutic strategies to restore immune regulation and slow type 1 diabetes (T1D) progression are in development and testing. A major challenge has been defining biomarkers to prospectively identify subjects likely to benefit from immunotherapy and/or measure intervention effects. We previously found that compared to healthy controls, Tregs from children with new-onset T1D have an altered Treg gene signature (TGS), suggesting this could be an immunoregulatory biomarker.

METHODS. nanoString was used to assess the TGS in sorted Tregs ($CD4^+CD25^{hi}CD127^{lo}$) or Peripheral Blood Mononuclear Cells (PBMC) from individuals with T1D or type 2 diabetes, healthy controls, or T1D recipients of immunotherapy. Biomarker discovery pipelines were developed and applied to various sample group comparisons.

RESULTS. Compared to controls, the TGS in isolated Tregs or PBMCs is altered in adult new-onset and cross-sectional T1D cohorts, with sensitivity and specificity of biomarkers increased by including T1D-associated single nucleotide polymorphisms in algorithms. The TGS was distinct in T1D versus type 2 diabetes, indicating disease-specific alterations. TGS measurement at the time of T1D onset revealed an algorithm that accurately predicted future rapid versus slow C-peptide decline, as determined by longitudinal analysis of placebo arms of […]

Treg gene signatures predict and measure type 1 diabetes trajectory

Anne M. Pesenacker[1,#], Virginia Chen[2], Jana Gillies[1], Cate Speake[3], Ashish K. Marwaha[4], Annika Sun[1], Samuel Chow[5], Rusung Tan[6], Thomas Elliott[7], Jan P. Dutz[5], Scott J. Tebbutt[2], Megan K. Levings[1*]

[1]Department of Surgery, University of British Columbia, and BC Children's Hospital Research Institute, Vancouver, BC, Canada

[2] Department of Medicine & Centre for Heart Lung Innovation, University of British Columbia, and Prevention of Organ Failure (PROOF) Centre of Excellence, St. Paul's Hospital, Vancouver, BC, Canada

[3] Diabetes Clinical Research Program, Benaroya Research Institute, Seattle, WA, USA

[4] Department of Molecular Genetics, University of Toronto, Toronto, ON, Canada

[5] Department of Dermatology and Skin Science, University of British Columbia, and BC Children's Hospital Research Institute, Vancouver, BC, Canada

[6] Department of Pathology, Sidra Medicine and Weill Cornell Medicine, Doha, Qatar

[7] Department of Medicine, University of British Columbia, and BCDiabetes, Vancouver, BC, Canada

[#] Effective July 2018: Division of Infection and Immunity, Institute of Immunity & Transplantation, University College London, London, United Kingdom

*Corresponding Author:
Megan K. Levings
A4-186, 950 West 28th Ave.
Vancouver, B.C. Canada
V5Z 4H4
+1 020 875 2000 x4686
mlevings@bcchr.ca

Conflict of interest: MKL has received research funding from TxCell, Pfizer and Bristol Myers Squibb and has patents pending on alloantigen specific chimeric antigen receptors. JPD has personal fees from Janssen, Abbvie, Amgen, Novartis, Leo, Celgene, Lilly and Pfizer. For UST1D (NCT02117765) Janssen provided vials of study drug in kind for a portion of the study and Sanofi provided in kind diabetes management supplies.

Abstract

Background: Multiple therapeutic strategies to restore immune regulation and slow type 1 diabetes (T1D) progression are in development and testing. A major challenge has been defining biomarkers to prospectively identify subjects likely to benefit from immunotherapy and/or measure intervention effects. We previously found that compared to healthy controls, Tregs from children with new-onset T1D have an altered Treg gene signature (TGS), suggesting this could be an immunoregulatory biomarker.

Methods: nanoString was used to assess the TGS in sorted Tregs ($CD4^{+}CD25^{hi}CD127^{lo}$) or Peripheral Blood Mononuclear Cells (PBMC) from individuals with T1D or type 2 diabetes, healthy controls, or T1D recipients of immunotherapy. Biomarker discovery pipelines were developed and applied to various sample group comparisons.

Results: Compared to controls, the TGS in isolated Tregs or PBMCs is altered in adult new-onset and cross-sectional T1D cohorts, with sensitivity and specificity of biomarkers increased by including T1D-associated single nucleotide polymorphisms in algorithms. The TGS was distinct in T1D versus type 2 diabetes, indicating disease-specific alterations. TGS measurement at the time of T1D onset revealed an algorithm that accurately predicted future rapid versus slow C-peptide decline, as determined by longitudinal analysis of placebo arms of START and T1DAL trials. The same algorithm stratified participants in a phase I/II clinical trial of ustekinumab (αIL-12/23p40) for future rapid versus slow C-peptide decline.

Conclusion: These data suggest that biomarkers based on measuring Treg gene signatures could be a new approach to stratify patients and monitor autoimmune activity in T1D.

Introduction

Insufficient FOXP3$^+$ regulatory T cell (Treg) control of T cell-mediated destruction of beta-cells likely contributes to type 1 diabetes (T1D) (1). Monogenic mutations in *FOXP3* resulting in a lack of functional Tregs lead to T1D (2) and several T1D risk alleles occur in Treg-associated genes (e.g. single nucleotide polymorphisms [SNPs] in *CD25*, *PTPN2* and *PTPN22*) (1). Accordingly, multiple studies are testing whether immunotherapy-based methods to boost Treg function can prevent or delay T1D progression (1, 3, 4). For example, inflammatory cytokine blockade (e.g. ustekinumab, αIL-12/23p40 (5)), co-stimulation targeting (e.g. alefacept, LFA3-4-Ig (6)), or Treg expansion (e.g. low-dose IL-2; cellular therapy (7, 8)) aim to restore the immunoregulatory balance. However, availability of clinically-applicable tests to measure changes in immunity during such trials is limited (3), with an on-going search for biomarkers to stratify patients likely to respond to a given therapy and track changes in immune regulation (4, 9).

We previously developed a composite biomarker assay which measures expression of 37 genes and discriminates between Tregs and conventional T cells (Tconvs) regardless of activation state and showed that Tregs from pediatric new onset T1D patients have a significantly altered gene signature (10). Here we tested whether Treg gene signatures (TGS) could also identify Treg alterations in adults with T1D and investigated the predictive power of TGS-based biomarkers to predict the rate of C-peptide decline.

Results

Adults with T1D have an altered Treg gene signature in sorted Tregs and PBMCs

We previously found that pediatric new onset T1D Tregs had a significantly different TGS compared to healthy children (10) and first tested if this was also true in adults. Tregs ($CD4^+CD25^{hi}CD127^{lo}$) were isolated from young adults with new onset T1D (18-35 years of age, <100 days after diagnosis, n=20, Figure 1A), a cross-sectional T1D cohort ((9), n=40, Figure 1B), or age- and sex-matched healthy controls (HC, n=10 or n=37). Expression of the TGS was measured using a nCounter FLEX and biomarker discovery analysis applied. We found the TGS distinguished between T1D and healthy Tregs with high AUCs [area under the receiving operating characteristic curves] in both cohorts (Figure 1A&B, AUC=0.830, =0.953). Cut-offs for sensitivity (true positives) and specificity (true negatives) determination were set between 0.25 and 0.75, revealing high sensitivity and specificity for both cohorts.

Genetic risk alleles including SNPs in *CD25*, *PTPN2* and *PTPN22* are associated with CD25 expression, response to IL-2, FOXP3 stability, and Treg function in T1D (1). We thus hypothesized that genotype information might refine biomarker accuracy. Biomarker discovery using the cross-sectional T1D cohort and including genotype(s) revealed that while overall AUCs were similar to those obtained without genotype, there was slightly improved sensitivity in several cases (Figure 2). For example, adding CD25 rs2104286 number of disease variants [NDV] improved the sensitivity from 0.875 (Figure 1B) to 0.950 (Figure 2C), but overall inclusion of SNPs only modestly improved accurate discrimination between healthy and T1D Tregs.

Clinical application of biomarker tests should ideally entail minimal sample processing to simplify implementation, reduce processing errors, and increase reproducibility. We therefore next examined whether differential TGS expression could be detected in unfractionated PBMCs. Gene expression in PBMC lysates from adult new onset (n=19, Figure 3A) and cross-sectional (n=35, Figure 3B) T1D cohorts, and age- and sex-matched controls (HC, n=10 or n=38) were measured and biomarker discovery analysis applied. Surprisingly, gene expression in PBMC lysates also revealed highly sensitive and specific algorithms that discriminated between healthy controls and new onset or cross-sectional T1D cohorts (AUC= 0.895, =0.977, respectively). Adding genotype information to biomarker discovery generated near perfect classification of T1D versus HCs with most AUCs, sensitivity and specificity >0.900 (Figure 4). Thus, the inclusion of Treg-associated SNPs is valuable when assessing changes in the overall immunoregulatory balance by measuring the TGS in PBMC lysates.

Differences in gene usage between Treg and PBMC-derived algorithms

The varying number and identity of genes in each best-performing algorithm led us to compare gene usage across algorithms derived from Tregs versus PBMCs in the cross-sectional T1D cohort (Figure 5). We found that there were 10 core genes in all of the best performing algorithms derived from sorted Tregs (Figure 5A). These included genes associated with DNA accessibility (*METTL7A*, a methyltransferase), transcription (*ZNF532*, *VAV3, RBMS3*), translation (*RPL23A*, a ribosomal protein), signal transduction (*VAV3*, TCR mediated signalling (11)), and cytokine receptors (*CSF2RB, IL1R1, IL7R*).

Examination of the PBMC-based algorithm also revealed 10 core genes (Figure 5B), with notable similarities and differences to the Treg-derived algorithms. For example, *FOXP3*

(significantly lower expression in PBMC T1D versus controls, p=0.0034, data not shown) and *TRIB1* (significantly higher expression in PBMC T1D versus controls, p<0.0001, data not shown) were included in all PBMC-based algorithms, but not in any derived from sorted Tregs. In contrast, *IL1RN* and *RPL23A* were always present in both Treg- and PBMC-based algorithms. Hence, PBMC-based algorithms may detect changes in Treg to Tconv ratios which are eliminated when analysing TGS of sorted Tregs.

Treg gene signature algorithms in type 1 versus type 2 diabetes

TGS changes could be related to poor glucose homeostasis rather than a change in immune regulation. We thus measured the TGS in sorted Tregs or PBMCs from type 2 diabetes (T2D) patients, and re-ran the age- and sex-matched T1D and HC lysates in parallel, in this case using the nCounter SPRINT system. Principle Components Analysis (PCA) was performed separately on Treg and PBMC data to highlight differences between patients (i.e. HC vs T1D vs T2D) rather than reiterate differences present between sample types (i.e. Tregs vs PBMCs). Analysis of the unweighted TGS revealed distinct clustering of T2D, T1D and HCs for both Treg and PBMC samples (Figure 6).

For these experiments, since we re-ran T1D and HC cohort samples from Figures 1&3 with the T2D samples on the nCounter SPRINT system we also had to opportunity to test T1D versus HC algorithms from Figure 1B “off-the-shelf”, finding excellent replication of the AUC (=1.000) and, without changing cut-offs, perfect sensitivity (=1.000) but low specificity (=0.222, Figure 7A). New biomarker analysis comparing T1D to T2D, or T2D to HC using Treg lysates also revealed algorithms that were highly sensitive and specific (AUCs >0.9, Figure 7B&C). Similar results were obtained when PBMC lysates were analysed. "Off-the-shelf" application of

the algorithm from Figure 3B revealed a high AUC (=0.922) and sensitivity (=0.900), but low specificity (=0.444, Figure 7D). As with sorted Tregs, new biomarker discovery in PBMCs also revealed distinct gene expression in T1D versus T2D, and between T2D and healthy controls (Figure 7 E&F). Each cohort comparison was defined by distinct sets of genes (Figure 7G&H), indicating there are intrinsic and extrinsic differences in Treg biology in T1D, T2D and HCs.

Application of the Treg gene signature as clinical trial monitoring tool.

A limitation of T1D disease management and clinical trials is the lack of non-invasive biomarkers to predict C-peptide trajectory and measure intervention benefit (9). Hence, we asked whether the TGS might predict disease trajectory. Together with the JDRF Biomarker Working Group and the Immune Tolerance Network, we obtained longitudinal samples from the placebo arms of the T1DAL and START trials (9). Subjects were divided into tertiles with slow, moderate or rapid C-peptide decline, as determined by mixed meal tolerance tests (MMTTs), according to absolute change in C-peptide levels from baseline (<100 days after diagnosis) to 24 months later (Figure 8A)

We measured the TGS in Treg and PBMC lysates from month 0 samples and performed biomarker discovery, seeking an algorithm that could predict future rapid versus slow C-peptide decline. Although the sample size was small (n=7 rapid vs 9 slow decline), the TGS in Treg lysates predicted C-peptide decline with an AUC=0.730 (Figure 8B). Subjects with a moderate rate of C-peptide decline showed an intermediate biomarker score. Furthermore, plotting normalized gene expression of month 0 Treg lysates showed trends in line with C-peptide decline (Figure 8C). Specifically, expression of all 4 genes incorporated in the algorithm either increased (*C8ORF70, PMSL11, STAM)* or decreased (*ICA1*) with progressively worse future C-

peptide decline. Expression of 2 additional genes not incorporated in the algorithm, *ID2* and *ZBTB38* also showed trends in line with C-peptide decline. In contrast, biomarker analysis of PBMC lysates was ineffective at discriminating between these groups (data not shown), suggesting that Treg-intrinsic alterations rather than an overall change in immunoregulatory balance may be better able to predict future disease course.

Finally, we tested if the TGS could predict C-peptide decline in the setting of immunotherapy. Specifically, we used samples from a phase I/II safety trial of ustekinumab (αIL-12/23 p40) in adult new onset T1D (NCT02117765). Ustekinumab is commonly used in psoriasis and inflammatory bowel disease (12), and its ability to block IL-12 and IL-23 might restore the abnormal balance of T helper subsets, and/or IL-17-producing Tregs that we (13) and others (14, 15) previously described in T1D. C-peptide was measured by MMTTs pre-treatment (month 0), and at 1 and 12 months after ustekinumab treatment. Subjects were divided into slow (n=11) or rapid (n=5) C-peptide decline based on reported expected rates of decline (16) (Figure 9A). We first applied the unmodified algorithm from Figure 8B "off-the-shelf" to pre-treatment Treg gene expression data finding this algorithm prospectively identified rapid versus slow C-peptide decline with AUC=0.709; however, the specificity was low (=0.182, Figure 9B), indicating that cut-offs for sensitivity/specificity calculations need refinement.

We then asked whether the TGS changed over the course of ustekinumab therapy by dividing month 9 Treg gene expression data by pre-treatment (month 0) data. Biomarker discovery revealed excellent predictive models (AUC=0.818, sensitivity=0.909 and specificity=0.800) that identified subjects with slow versus rapid C-peptide decline (Figure 9C). Evidence that the algorithm improved when both pre-treatment and month 9 data were included suggests that subjects with sustained versus rapidly declining C-peptide may have differing

ustekinumab-driven changes in their TGS. As with the non-interventional longitudinal samples, algorithms based on month 0 PBMC lysates were ineffective (data not shown).

Finally, the TGS at month 9 could also differentiate between slow and rapid C-peptide decline (Figure 9D&E). Interestingly, at this time point both Treg and PBMC-derived signatures yielded good algorithms (AUCs=0.900 and =0.745, respectively, Figure 9D&E). These data suggest that the TGS may detect ustekinumab-mediated changes in Treg-intrinsic gene expression and in the balance between Tregs and Tconvs upon immunotherapy. We found some gene usage overlap with algorithms described in previous Figures (Figure 9F).

Discussion

Here we build on our previous finding that Tregs from children with new-onset T1D have an altered TGS and show that this is also true in adult new-onset and cross-sectional T1D cohorts. The altered T1D TGS did not appear to be determined to changes in glucose homeostasis as analysis of samples from subjects with type 2 diabetes revealed no overlap in gene expression profiles. We also showed the potential of TGS monitoring as a biomarker of disease trajectory, possibly enabling patient stratification for immunotherapy and monitoring of therapy outcomes. TGS measurement is simple, requires very small amounts of blood and integrates multiple aspects of Treg biology that would be difficult to quantify in individual assays.

Our biomarker discovery approach utilized a leave one out cross validation approach to identify algorithms with high AUCs, sensitivity and specificity for each comparison of interest with the resulting algorithms typically only including a subset of the 37 quantified transcripts. Comparisons between different algorithms revealed interesting trends in transcript utilization in samples of sorted Tregs versus PBMCs. For example, analysis of gene expression in sorted Tregs

revealed recurring cell surface receptors and cell signalling molecules, suggesting that T1D Tregs have intrinsic differences in their capability to interpret and transmit molecular signals. In contrast, evidence that one of the most differentially expressed gene in PBMC-based algorithms was *FOXP3*, suggests that these samples detect changes in Treg to Tconv ratios. This possibility is supported by the finding that *FOXP3* was not present in algorithms derived from sorted Tregs; samples in which differential ratios between Treg to Tconv are eliminated.

Despite small sample sizes, we found that the TGS may be a novel approach to the long-standing challenge of predicting and measuring T1D disease trajectory and intervention effects on the immunoregulatory balance. Specifically, application of a single TGS algorithm in two independent cohorts was able to identify the majority of new onset T1D subjects whose C-peptide was likely to decline rapidly. Interestingly, pre-existing changes in Tregs seemed to correlate with future disease trajectory after ustekinumab treatment. These findings may indicate that a Treg-specific defect, instead of an immunoregulatory-imbalance, dictates future disease course. Our data also suggest possible differential ustekinumab-mediated intrinsic effects on Tregs and the immunoregulatory-balance in subjects with rapid versus slow C-peptide decline. Overall these data indicate that further testing of TGS-based algorithms in larger cohorts is warranted.

To date, only two other studies have reported prognostic biomarkers after T1D onset. Hessner et al measured changes in PBMC gene expression upon culture in T1D plasma (17), finding that patients with higher inflammatory signature at baseline had slower C-peptide decline in response to IL-1RA in the AIDA trial (NCT00711503). Similarly, Linsley et al employed whole blood RNA-sequencing to find an increased T cell signature early after rituximab (NCT00279305) in patients with rapid C-peptide decline after 1 year (18). Compared to these

large "omic" based approaches, nanoString-based TGS measurement requires very few cells (<10,000) and minimal processing, making it easier to test in validation studies and more clinically feasible. As our understanding of T1D evolves from a linear to a relapsing-remitting autoimmunity model (19), it will be of interest to continue measuring the TGS prospectively over time, including before disease diagnosis, to determine if it may enable real-time evaluation of autoimmune activity.

In conclusion, these findings suggest that measuring Treg gene signatures could be a step towards a biomarker of immune status in T1D. Future application of our findings across multiple studies together with development of a cross-platform and cross-chemistry standardization workflow may lead to the development of "universal" algorithms that could be applied to identify rapid vs slow progressors, monitor T1D over time, and/or select subjects likely to respond to immunotherapy.

Methods

Sample collection and cell isolation. Peripheral blood from each cohort was obtained and cryopreserved as PBMCs (Supplemental Tables T1-5). Upon thawing, a proportion of each sample was used to isolate Tregs (sorted as $CD4^{+}CD25^{hi}CD127^{lo}$ cells, antibody information in supplemental Tables T6 & T7). Sorted Tregs and PBMCs were both lysed in RLT lysis buffer (Qiagen) at 3,500-5,000 cells/μL.

nanoString analysis. mRNA expression was measured in 2μL Treg/PBMC lysates with a custom nCounter reporter probe set on nanoString nCounter FLEX or SPRINT systems. Sample quality was assessed by cartridge-specific normalization factors and positive control linearity. Gene expression data were normalized in four steps: 1) multiplication by sample's normalization factor (geometric mean of positive controls divided by median); 2) total sum normalization equalling 5000 counts; 3) log2 transformation; and 4) ComBat batch correction (20). Each cohort, PBMCs or Tregs were batch-corrected separately.

Statistics. Analyses were performed using R (21) and GraphPad Prism V8. Biomarker discovery analysis included 31 TGS genes (10) plus 6 genes differentially expressed between healthy and T1D. Differential expression was assessed using LiMMa (22) with p-value threshold of 0.1. Binary classifiers were built using logistic or elastic net regression (23), with α=0.65 (10) or =0.9. Where genotypes were available, the number of disease variant alleles (NDV) for each patient (either for a single SNP, or all eight SNPs tested) was included in the analysis as a covariate. Leave-one-out cross-validation was used to obtain performance estimates (area under the receiving operating characteristic curve (AUC), sensitivity, and specificity). For each

comparison, the best algorithm was selected on the basis of the highest AUC. To define sensitivity (true positive) and specificity (true negative), the definition of the cut-off for samples falling into one group versus another was set between 0.25 and 0.75 and is indicated by a dotted line on each biomarker score graph.

Comparison of two groups was performed by unpaired t-test (referenced in text, data not shown) and of multiple groups was performed by one-way ANOVA with Tukey's multiple comparisons test (Figure 8C) and a p value of 0.05 was considered significant (data in 8C was not significantly different) using GraphPad Prism V8.

Study approval. Protocols were approved by Clinical Research Ethics Boards of University of British Columbia, Benaroya Research Institute, and under the auspices of approved clinical trial protocols: UST1D (NCT02117765), START (NCT00515099 (24)) and T1DAL (NCT00965458 (6)). Consort flow diagrams for the respective trials are shown in Supplemental Figures S1-3.

Author Contributions

AMP contributed to the overall study design, execution of the experiments, and writing of the manuscript. VC performed bioinformatic and statistical analysis. JG assisted in Treg sorting and running nanoString Sprint system. CS oversaw subject recruitment, sample biobanking and patient data collection for the cross sectional T1D and T2D cohorts; she applied for and received longitudinal T1D samples and patient data from the ITN (placebo arms START, T1DAL trials). CS oversaw Treg sorting for the cross sectional T1D and longitudinal ITN samples. AKM, AS, SC, TE, JPD oversaw subject recruitment, sample biobanking and patient data collection for ustekinumab trial samples, with AKM, AS, SC as study coordinators, and JPD, RT, TE and MKL principal or co-investigators. SJT supervised bioinformatic and statistical analysis and contributed to study design. MKL contributed to the overall design and execution of the research and writing of the manuscript and takes responsibility for the content of the article.

Acknowledgements

The authors thank the BC Children's Hospital biobank for subject recruitment and sample processing, Constadina Panagiotopoulos (BC Children's Hospital Research Institute [BCCHRI] and University of British Columbia (UBC)) for contributions to the diabetes biobank, and Paul C. Orban and C. Bruce Verchere (BCCHRI and UBC) for ongoing support and discussions. We acknowledge Dr. Marla Inducil (BCDiabetes) for her tireless work in coordinating the ustekinumab trial (NCT02117765). The authors thank Carla Greenbaum, Kevin St. Jacques, Kristy Meyer, Daxa Sabhaya, Katrina Dziubkiewicz, Mary Ramey, Heather Vendettuoli, Jani Klein, McKenzie Lettau (Benaroya Research Institute [BRI]) for sample collection at BRI, Janice Chen for technical assistance, and Gerald Nepom, Elisavet Serti and Kristina Harris from

the ITN for their support. We also thank the PROOF Centre of Excellence and UBC Centre for Heart Lung Innovation teams for valuable discussions, as well as Basak Sahin for technical assistance on nCounter FLEX assays.

Research reported in this publication was supported by grants from JDRF (1-PNF-2015-113-Q-R, 2-PAR-2015-123-Q-R, and 3-SRA-2016-209-Q-R), the JDRF Canadian Clinical Trials Network (CCTN), and National Institute of Allergy and Infectious Diseases of the National Institutes of Health under Award Numbers UM1AI109565 and FY15ITN168. The content is solely the responsibility of the authors and does not necessarily represent the official views of the National Institutes of Health. For UST1D (NCT02117765) Janssen provided vials of study drug in kind for a portion of the study and Sanofi provided in kind diabetes management supplies. AMP was supported by fellowships from JDRF and the JDRF CCTN. MKL receives a Scientist Salary Award from the BCCHRI.

References

1. Hull CM, Peakman M, and Tree TIM. Regulatory T cell dysfunction in type 1 diabetes: what's broken and how can we fix it? *Diabetologia.* 2017;60(10):1839-50.
2. Bacchetta R, Barzaghi F, and Roncarolo MG. From IPEX syndrome to FOXP3 mutation: a lesson on immune dysregulation. *Annals of the New York Academy of Sciences.* 2016.
3. Greenbaum C, Lord S, and VanBuecken D. Emerging Concepts on Disease-Modifying Therapies in Type 1 Diabetes. *Current diabetes reports.* 2017;17(11):119.
4. Frumento D, Ben Nasr M, El Essawy B, D'Addio F, Zuccotti GV, and Fiorina P. Immunotherapy for type 1 diabetes. *Journal of endocrinological investigation.* 2017;40(8):803-14.
5. Marwaha AK, Tan S, and Dutz JP. Targeting the IL-17/IFN-gamma axis as a potential new clinical therapy for type 1 diabetes. *Clin Immunol.* 2014;154(1):84-9.
6. Rigby MR, DiMeglio LA, Rendell MS, Felner EI, Dostou JM, Gitelman SE, et al. Targeting of memory T cells with alefacept in new-onset type 1 diabetes (T1DAL study): 12 month results of a randomised, double-blind, placebo-controlled phase 2 trial. *Lancet Diabetes Endocrinol.* 2013;1(4):284-94.
7. Klatzmann D, and Abbas AK. The promise of low-dose interleukin-2 therapy for autoimmune and inflammatory diseases. *Nature reviews.* 2015;15(5):283-94.
8. Bluestone JA, Buckner JH, Fitch M, Gitelman SE, Gupta S, Hellerstein MK, et al. Type 1 diabetes immunotherapy using polyclonal regulatory T cells. *Sci Transl Med.* 2015;7(315):315ra189.
9. Speake C, and Odegard JM. Evaluation of Candidate Biomarkers of Type 1 Diabetes via the Core for Assay Validation. *Biomark Insights.* 2015;10(Suppl 4):19-24.
10. Pesenacker AM, Wang AY, Singh A, Gillies J, Kim YW, Piccirillo CA, et al. A Treg gene signature is a specific and sensitive biomarker to identify children with new onset type 1 diabetes. *Diabetes.* 2016.
11. Tybulewicz VL, Zakaria S, Gomez TS, Savoy DN, McAdam S, Turner M, et al. Vav-family proteins in T-cell signalling. *Current opinion in immunology.* 2005;17(3):267-74.
12. Elliott M, Benson J, Blank M, Brodmerkel C, Baker D, Sharples KR, et al. Ustekinumab: lessons learned from targeting interleukin-12/23p40 in immune-mediated diseases. *Annals of the New York Academy of Sciences.* 2009;1182:97-110.
13. Marwaha AK, Crome SQ, Panagiotopoulos C, Berg KB, Qin H, Ouyang Q, et al. Cutting edge: Increased IL-17-secreting T cells in children with new-onset type 1 diabetes. *J Immunol.* 2010;185(7):3814-8.
14. Honkanen J, Nieminen JK, Gao R, Luopajarvi K, Salo HM, Ilonen J, et al. IL-17 immunity in human type 1 diabetes. *J Immunol.* 2010;185(3):1959-67.
15. Arif S, Moore F, Marks K, Bouckenooghe T, Dayan CM, Planas R, et al. Peripheral and islet interleukin-17 pathway activation characterizes human autoimmune diabetes and promotes cytokine-mediated beta-cell death. *Diabetes.* 2011;60(8):2112-9.
16. Greenbaum CJ, Beam CA, Boulware D, Gitelman SE, Gottlieb PA, Herold KC, et al. Fall in C-peptide during first 2 years from diagnosis: evidence of at least two distinct phases from composite Type 1 Diabetes TrialNet data. *Diabetes.* 2012;61(8):2066-73.
17. Cabrera SM, Wang X, Chen YG, Jia S, Kaldunski ML, Greenbaum CJ, et al. Interleukin-1 antagonism moderates the inflammatory state associated with Type 1 diabetes during

clinical trials conducted at disease onset. *European journal of immunology.* 2016;46(4):1030-46.
18. Linsley PS, Greenbaum CJ, Rosasco M, Presnell S, Herold KC, and Dufort MJ. Elevated T cell levels in peripheral blood predict poor clinical response following rituximab treatment in new-onset type 1 diabetes. *Genes and immunity.* 2018;in press.
19. Li X, Cheng J, and Zhou Z. Revisiting multiple models of progression of beta-cell loss of function in type 1 diabetes: Significance for prevention and cure. *Journal of diabetes.* 2016;8(4):460-9.
20. Johnson WE, Li C, and Rabinovic A. Adjusting batch effects in microarray expression data using empirical Bayes methods. *Biostatistics.* 2007;8(1):118-27.
21. Team RC. R: A Language and Environment for Statistical Computing. http://www.R-project.org. 2014.
22. Ritchie ME, Phipson B, Wu D, Hu Y, Law CW, Shi W, et al. limma powers differential expression analyses for RNA-sequencing and microarray studies. *Nucleic Acids Res.* 2015;43(7):e47.
23. Zou H, and Hastie T. Regularization and variable selection via the elastic net. *Journal of the Royal Statistical Society: Series B (Statistical Methodology).* 2005;67(2):301-20.
24. Gitelman SE, Gottlieb PA, Felner EI, Willi SM, Fisher LK, Moran A, et al. Antithymocyte globulin therapy for patients with recent-onset type 1 diabetes: 2 year results of a randomised trial. *Diabetologia.* 2016;59(6):1153-61.

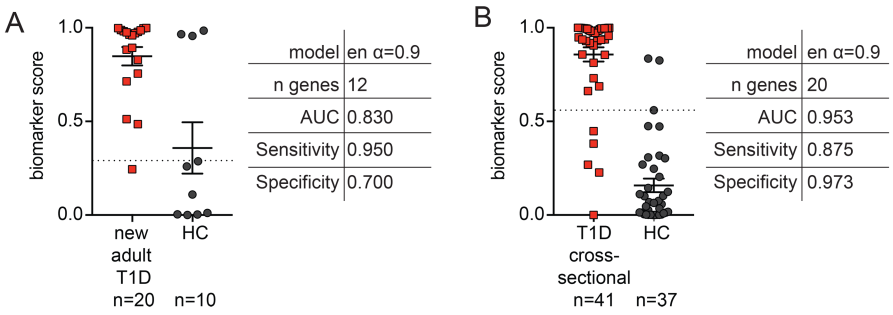

Figure 1. ***Altered intrinsic Treg gene signature in adults with T1D***. $CD25^{hi}CD127^{lo}$ Tregs were sorted from (A) adult new onset T1D (n=20) or (B) a cross-sectional T1D cohort (n=41) and age- and sex-matched controls (n=10 for A, or =37 for B). The Treg gene signature in the resulting lysates was measured on the nCounter FLEX platform. Biomarker scores and details (model of biomarker analysis selected [en, elastic net], number [n] of genes, AUC, sensitivity and specificity) for the best algorithm differentiating between T1D and healthy are indicated next to biomarker score dot-plots. Horizontal lines represent means with SD as error bars; dashed horizontal lines represent cut-offs for sensitivity and specificity calculations.

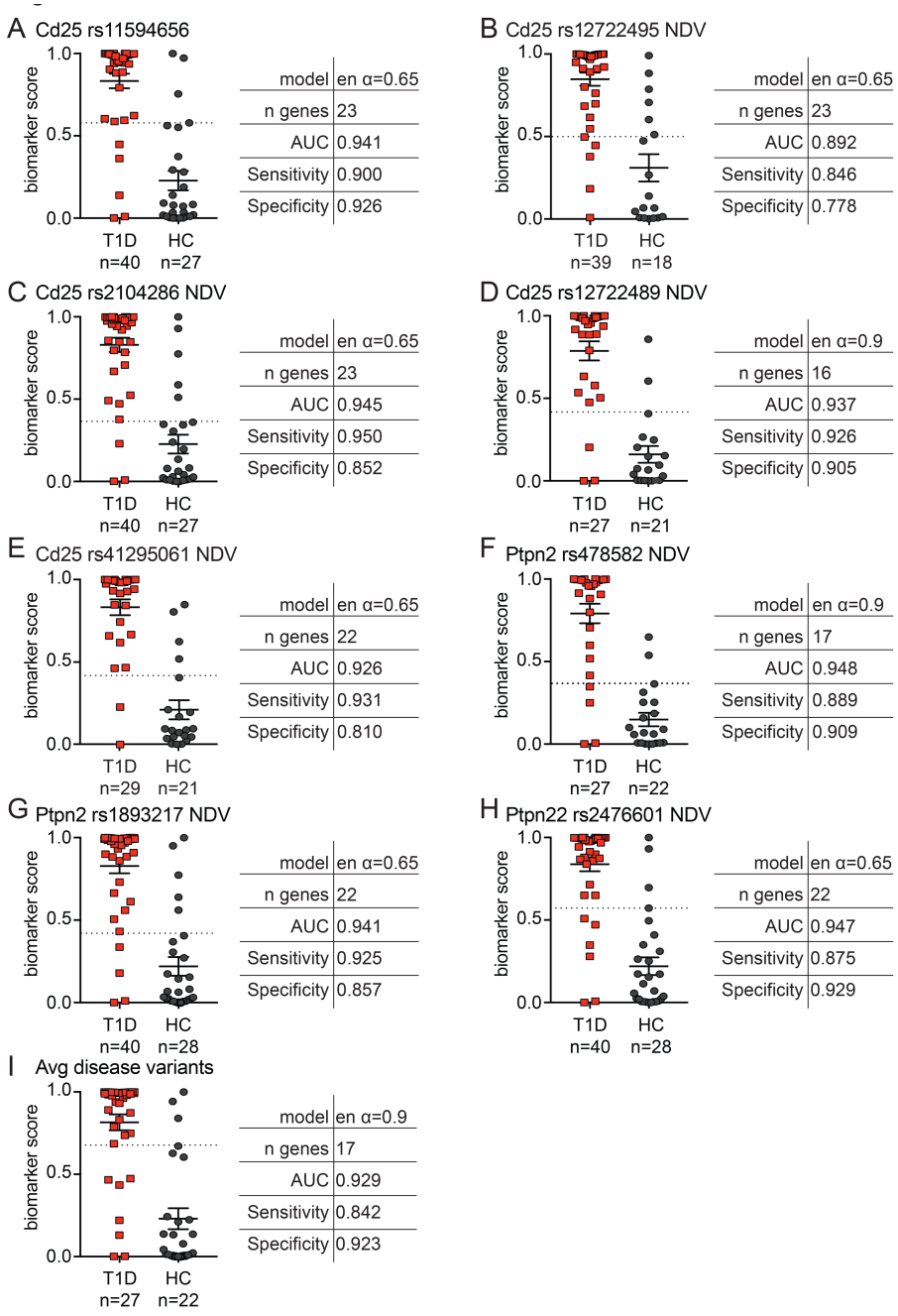

Figure 2. ***Addition of Treg-associated T1D SNPs enhances sensitivity of Treg-based algorithms.*** New algorithms were created using combinations of the gene signature data from sorted Tregs (cross sectional T1D and healthy cohorts) and a single indicated SNP genotype included as categorical value (i.e. each genotype given a specific weight) or as the number of disease variants/alleles (NDV) (i.e. 0, 1, or 2) encoding the indicated SNP. Shown are the best algorithms for each SNP: (A) genotype included as categorical value and (B-H) included as NDVs. (I) Biomarker score and algorithm for gene signature data combined with the average number of (Avg) disease variants for all SNPs assessed in A-H. Horizontal lines represent means with SD as error bars; dashed horizontal lines represent cut-offs for sensitivity and specificity calculations.

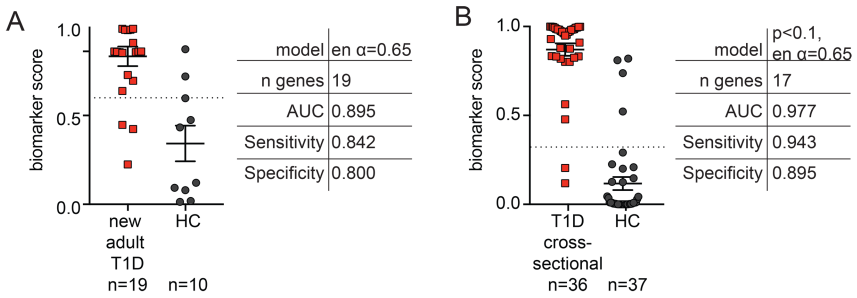

Figure 3. ***Detection of an altered Treg gene signature in PBMCs from adults with T1D***. The Treg gene signature was measured in PBMCs from (A) adult new onset T1D (n=19) or (B) a cross-sectional T1D cohort (n=36) and age- and sex-matched controls (n=10 for A, or =37 for B). Biomarker scores and details (as described in Figure 1; [p<0.1, cut-off for differential gene expression included in the biomarker discovery analysis; glm, generalized linear model]) for the best algorithm differentiating between T1D and healthy are indicated next to biomarker score dot-plots. Horizontal lines represent means with SD as error bars; dashed horizontal lines represent cut-offs for sensitivity and specificity calculations.

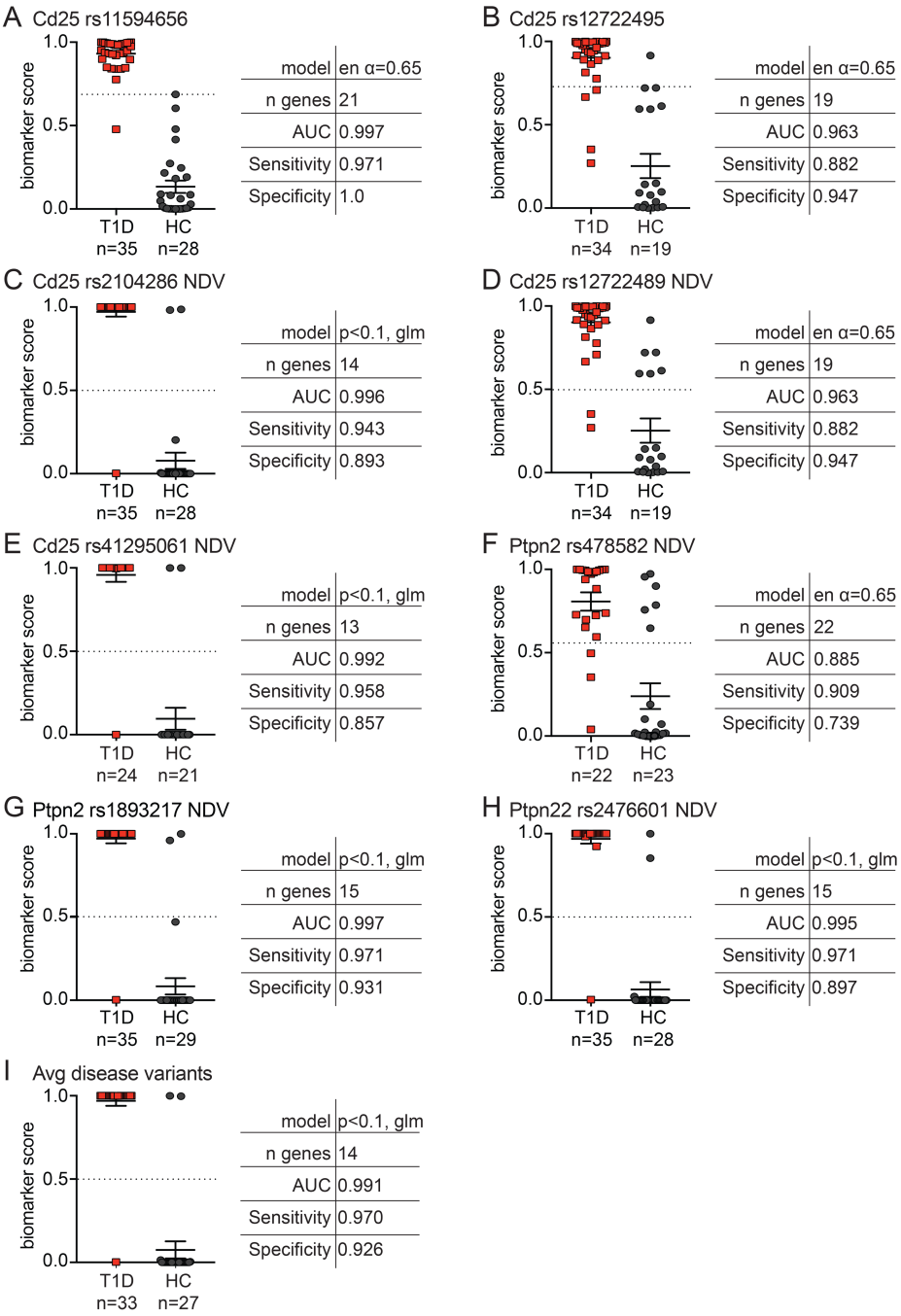

Figure 4. ***Addition of Treg-associated T1D SNPs enhances sensitivity of PBMC-based algorithms.*** New algorithms were created using combinations of gene signature data from PBMCs (isolated from cross sectional T1D and healthy cohorts) and a single indicated SNP genotype included as categorical value (i.e. each genotype given a specific weight) or as the number of disease variants/alleles (NDV) (i.e. 0, 1, or 2). (A&B) genotype included as categorical value and (C-H) genotype included as NDVs. (I) Biomarker scores and algorithm details combining gene signature data and the average number of (Avg) disease variants across all SNPs assessed. Horizontal lines represent means with SD as error bars; dashed horizontal lines represent cut-offs for sensitivity and specificity calculations.

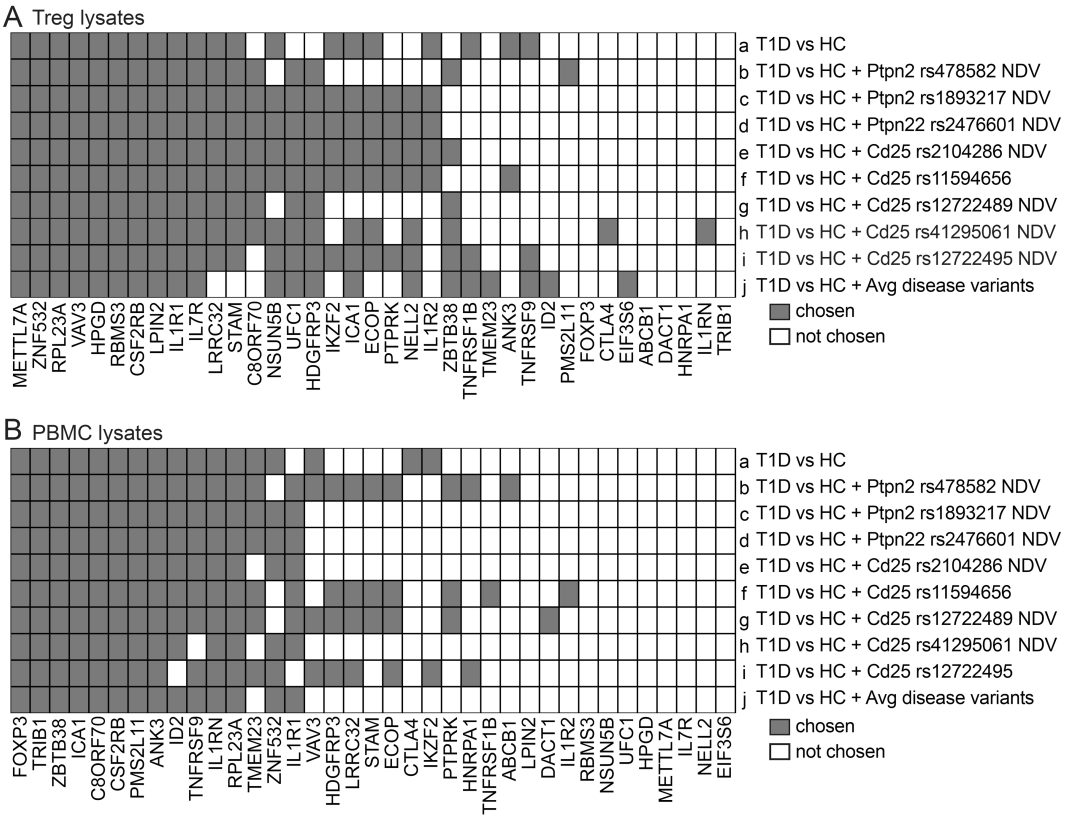

Figure 5. ***Differential gene usage in Treg versus PBMC-derived algorithms.*** Summary of which genes were present in the best performing algorithms from the cross-sectional T1D and healthy cohorts. (A) Treg-based algorithms described in Figure 1B and 2. (B) PBMC-based algorithms described in Figure 3B and 4. Each of the 37 mRNAs measured is listed, grey and white squares indicate genes which were or were not present in the best performing algorithm, respectively.

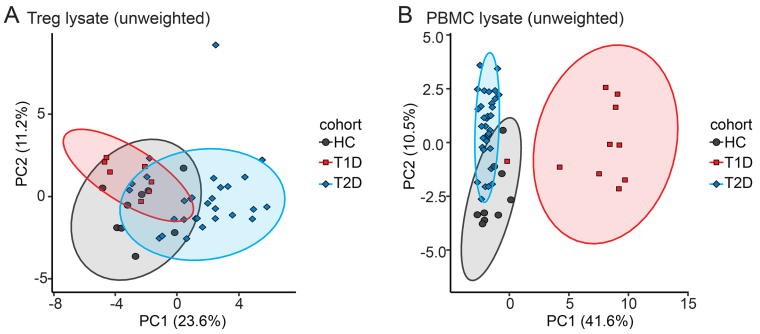

Figure 6. ***Altered Treg gene signature in type 2 diabetes (T2D) compared to T1D and healthy controls***. The Treg gene signature was measured in sorted CD25^{hi}CD127^{lo} Tregs and PBMCs from the indicated age- and sex-matched cohorts using the nCounter SPRINT system. For Tregs: T2D n=29, T1D n=7, and healthy controls (HC) n=9. For PBMCs: T2D n=33, T1D n=10, and healthy controls n=9. Shown is a principal component analysis representing expression of all 37 genes by sample group in (A) Tregs or (B) PBMCs. 95% confidence intervals are overlaid as ellipses.

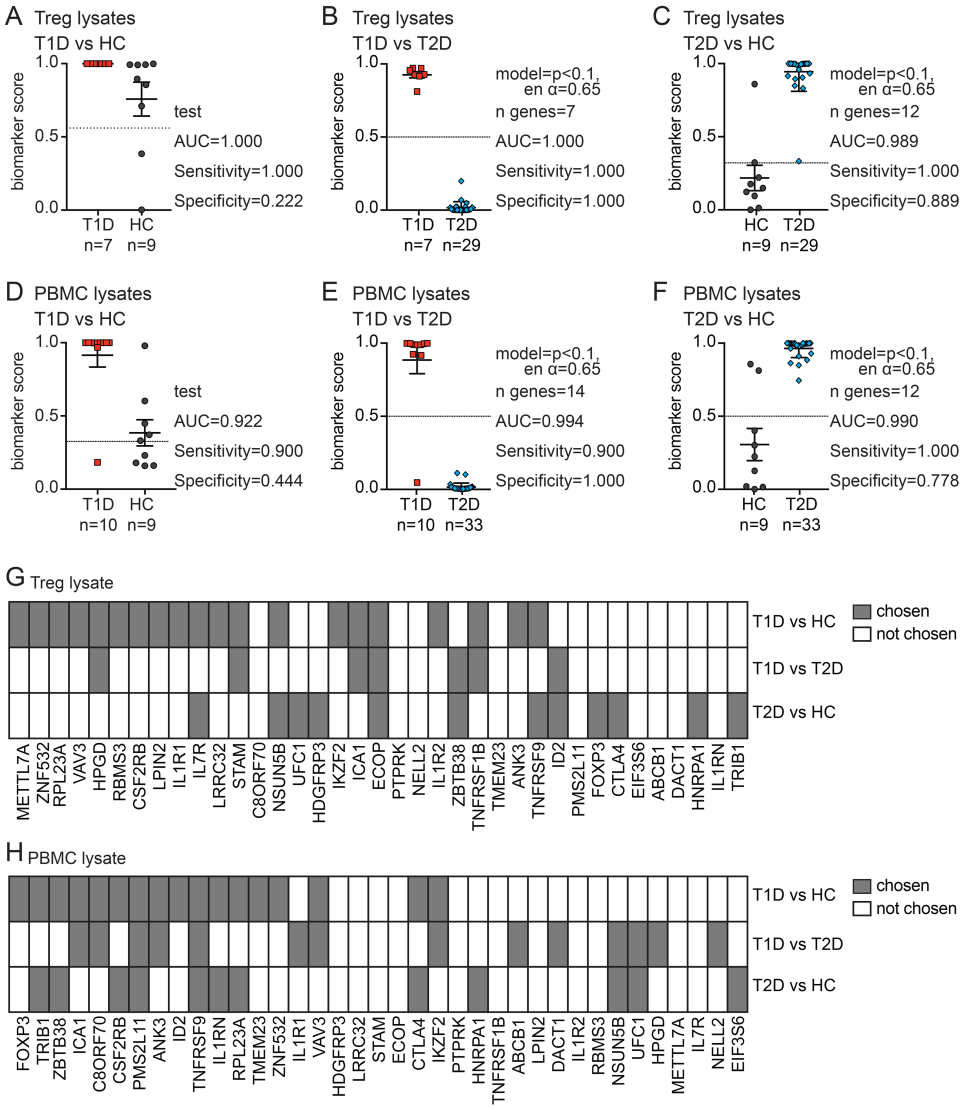

Figure 7. ***Treg gene signature algorithms differentiate type 1 or type 2 diabetes, and healthy controls.*** PBMC and Treg lysates from the indicated T1D or type 2 diabetes (T2D) cohorts were run on a nCounter SPRINT system together with age- and sex-matched healthy control samples. (A) Biomarker scores and performance when the algorithm from Figure 1B was applied to T1D and healthy control (HC) Treg data. (B&C) Biomarker scores and details (as described in Figure 1) of the best biomarker algorithm differentiating between Tregs from (B) T1D or (C) healthy controls and T2D samples. (D) Biomarker scores and performance when the algorithm from Figure 3B was applied to T1D and healthy control PBMC data. (E&F) Biomarker scores and details (as described in Figure 1&3) of the best biomarker algorithm differentiating between (E) T1D or (F) control and T2D samples in PBMCs. Horizontal lines represent means with SD as error bars; dashed horizontal lines represent cut-offs for sensitivity and specificity calculations. (G&H) Summary of gene usage in each (G) Treg or (H) PBMC-based algorithm described in A-F. Each of the 37 mRNAs measured is listed, grey and white squares indicate genes which were or were not present in the best performing algorithm, respectively.

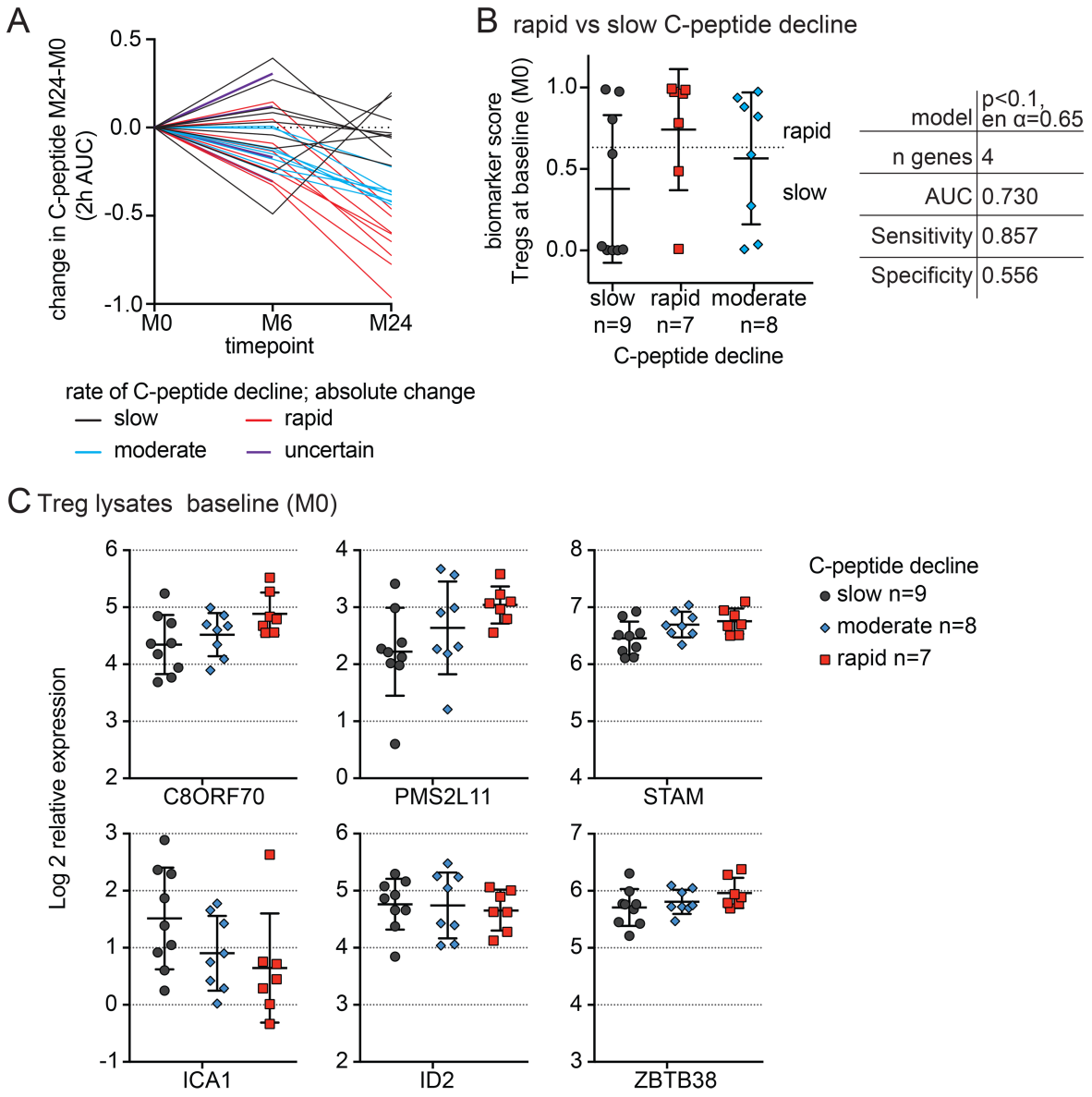

Figure 8. ***The Treg gene signature as a predictive biomarker of C-peptide decline.*** (A) C-peptide was quantified (2h AUC MMTT) in new onset T1D patients in the placebo arms of the T1DAL and START clinical trials (see CONSORT Flow Diagrams in Supplemental Figures S1&2) at baseline (M0), 6 months (M6) and 24 months (M24). The absolute change in C-peptide from M0 to M24 was calculated and subjects were divided into those with slow (n=9), moderate (n=8) or rapid (n=7) decline based on terciles. (B&C). Tregs ($CD4^{+}CD25^{hi}CD127^{lo}$) were sorted from cryopreserved PBMCs isolated from these subjects at baseline (M0) and the TGS was measured. (B) Biomarker score and details (as described in Figure 1&3) of the best algorithm predicting future rapid, slow, or moderate C-peptide decline. Horizontal lines represent means with SD as error bars; dashed horizontal lines represent cut-offs for sensitivity and specificity calculations. (C) Expression of the indicated genes plotted by rate of C-peptide decline group, with one-way ANOVA with Tukey's multiple comparisons test (* p-value ≤0.05, but data not significantly different).

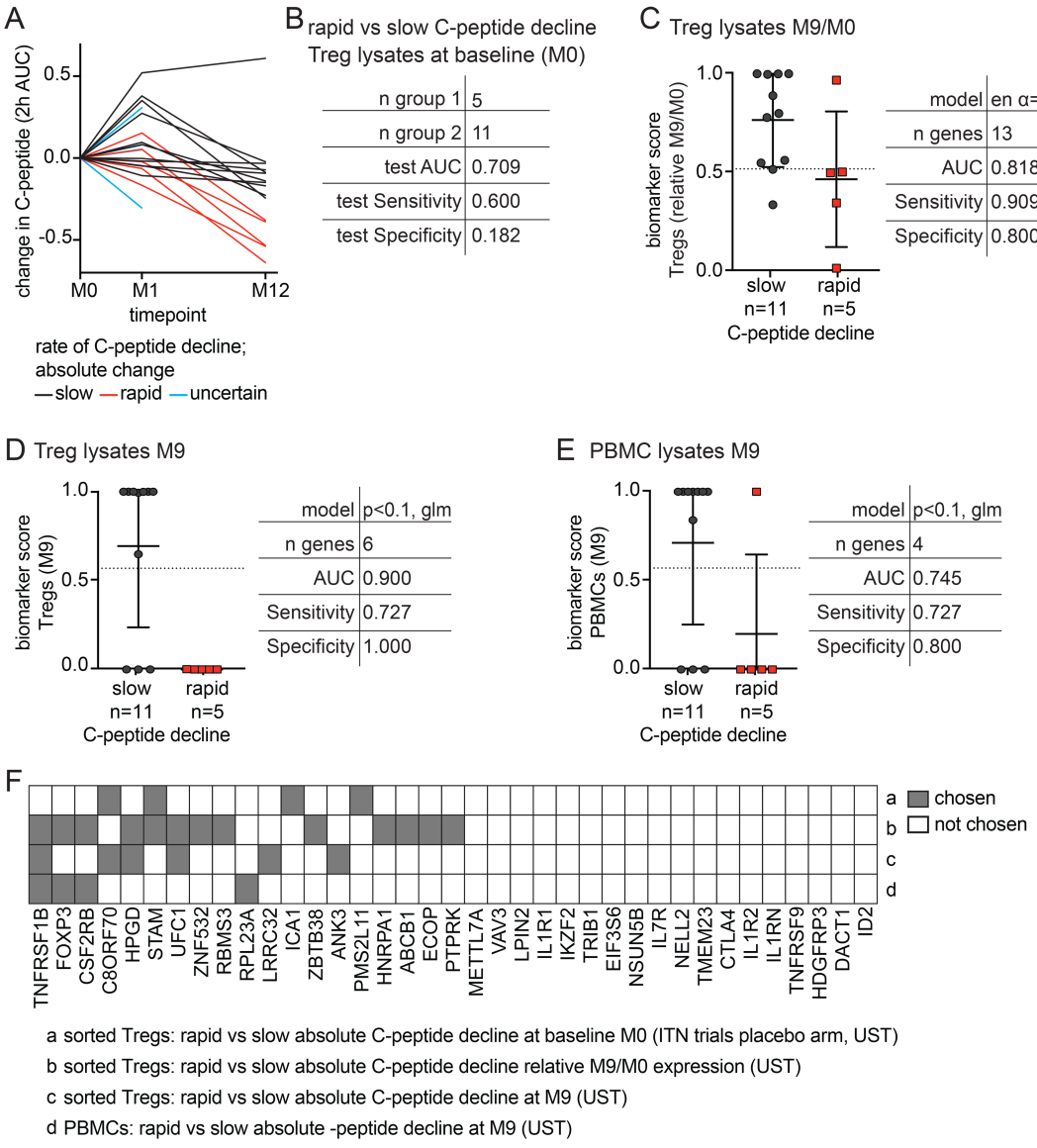

Figure 9. ***The Treg gene signature as a predictive biomarker of C-peptide decline in T1D subjects treated with ustekinumab.*** Adult new onset T1D patients were treated with ustekinumab as outlined in the CONSORT Flow diagram in Supplemental Figure S3. (A) C-peptide was quantified (2h AUC MMTT) at baseline (M0), 1 month (M1) and 12 months (M12), and absolute change in C-peptide from M0 to M12 was calculated. Subjects were divided into those with slow (n=11) or rapid (n=5) decline based on the absolute decline at M12, with slow subjects defined as those who lost less than 0.3pmol of C-peptide/year. (B-E) The TGS was measured in sorted $CD25^{hi}CD127^{lo}$ Tregs or PBMCs from M0 and M9 samples. (B) Test details when the algorithm from Figure 8B was applied to M0 Treg data. (C) Treg-based algorithm and biomarker scores for slow versus rapid C-peptide decline using relative TGS data (M9/M0 prior to log2 transformation). (D) Treg- and (E) PBMC-based algorithm and biomarker scores using M9 TGS expression data. Horizontal lines in (C-E) represent means with SD as error bars; dashed horizontal lines represent cut-offs for sensitivity and specificity calculations. (F) Summary of gene usage in c-peptide decline algorithms described in B-E.